Accepted Manuscript

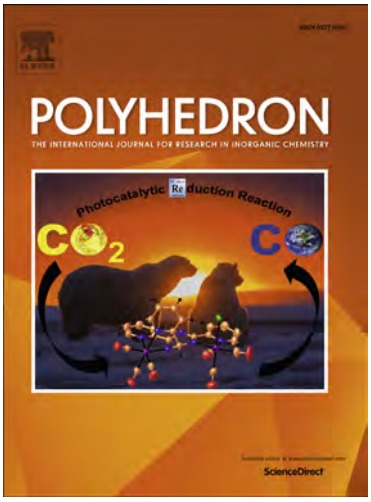

Synthesis and Reactivity of Phosphanido Bridged 1,1'-Bis(diphenylphosphino)ferrocene Complexes $[(R_F)_2Pt(\mu\text{-}PPh_2)_2M(dppf)]$ [M= Pt, Pd]

Daniela Giardina-Papa, Irene Ara, Susana Ibá ñez, Piero Mastrorilli, Vito Gallo, Juan Forniés

PII: S0277-5387(16)30191-7
DOI: http://dx.doi.org/10.1016/j.poly.2016.05.040
Reference: POLY 12014

To appear in: *Polyhedron*

Received Date: 17 March 2016
Accepted Date: 18 May 2016

Please cite this article as: D. Giardina-Papa, I. Ara, S. Ibáñez, P. Mastrorilli, V. Gallo, J. Forniés, Synthesis and Reactivity of Phosphanido Bridged 1,1'-Bis(diphenylphosphino)ferrocene Complexes $[(R_F)_2Pt(\mu\text{-}PPh_2)_2M(dppf)]$ [M= Pt, Pd], *Polyhedron* (2016), doi: http://dx.doi.org/10.1016/j.poly.2016.05.040

Synthesis and Reactivity of Phosphanido Bridged 1,1'-Bis(diphenylphosphino)ferrocene Complexes [$(R_F)_2Pt(\mu$-$PPh_2)_2M(dppf)$] [M= Pt, Pd]

Daniela Giardina-Papa,[a,b] Irene Ara,[a] Susana Ibáñez,[a] Piero Mastrorilli,*[b] Vito Gallo, and Juan Forniés*[a]

a Departamento de Química Inorgánica, Instituto de Síntesis Química y Catálisis Homogénea, Universidad de Zaragoza - CSIC, 50009 Zaragoza, Spain.

b Dipartimento di Ingegneria Civile, Ambientale del Territorio, Edile e di Chimica DICADECh del Politecnico di Bari, via Orabona 4, I-70125 Bari, Italy.

Polynuclear Homo- or Heterometallic Palladium(II)-Platinum(II) Pentafluorophenyl Complexes Containing Bridging Diphenylphosphido Ligands. 35. For part 34 see reference [1].

** Dedicated to Prof. Martin Bennet on the occasion of his 80th anniversary*

Keywords:
Palladium, Platinum, Phosphanides, polynucear complexes, metal-metal bonds.

ABSTRACT

Hetero-trinuclear complexes of formula [$(C_6F_5)_2Pt(\mu$-$PPh_2)_2M(dppf)$] [dppf = 1,1'-bis(diphenylphosphino)ferrocene, M = Pt (**1**), M = Pd (**2**)] were prepared by coupling between *cis*-[$(C_6F_5)_2Pt(PPh_2)_2$]Li_2 and *cis*-MCl_2(dppf). Reaction of the Pt/Pt/Fe species **1** with [$Ag(OClO_3)(PPh_3)$] or I_2 resulted in the formation of the complexes

$[(C_6F_5)(PPh_3)Pt(\mu\text{-}PPh_2)_2Pt(dppf)]$ (**3**) and $[(C_6F_5)(I)Pt(\mu\text{-}PPh_2)_2Pt(dppf)]$ (**4**), respectively, in which one of the pentafluorophenyl ligands has been replaced by PPh_3 or I. Reaction of the Pt/Pd/Fe species **2** with $Ag(ClO_4)$ afforded the tetranuclear complex $[(C_6F_5)_2Pt(\mu\text{-}PPh_2)_2Pd(dppf)Ag]$ (**5**) where the silver atom is bonded to Pd, to one of the bridging P and to one of the dppf P atoms. With $[Ag(OClO_3)(PPh_3)]$, complex **5** is also formed, although mixed with $[Ag(PPh_3)_2][ClO_4]$.A dynamic process in solution, in which the silver atom passes from one Pd–μPPh_2 bond to the other, has been observed at room temperature for complex **5**. The crystal structures of **3**, **4** and **5** are reported.

INTRODUCTION

The ability of diorganophosphanido ligands to stabilize polynuclear complexes is well known. The PR_2 group usually acts as bridging ligand and displays a great geometrical flexibility which allows to obtain M_2P moieties (M = metal centre) across a wide range of M–M distances [1-15].

We have started a project aimed at studying the reactivity of diorganophosphanido bridged Pt/Pt, Pd/Pd or Pt/Pd species towards silver based electrophiles and we found that the reaction course depends on *i*) the metal core; *ii*) the ancillary ligands of the polynuclear species; *iii*) the nature of the electrophile. The reaction products typically achieved by these reactions can be grouped in three categories: those deriving from metal oxidation, those resulting by pentafluorophenyl substitution and those displaying Ag-metal bonds (Scheme 1). For example, reaction of the complex $[NBu_4]_2[(C_6F_5)_2Pt(\mu\text{-}PPh_2)_2Pt(C_6F_5)_2]$ with $AgClO_4$ [16] results in the metal oxidation with formation of the Pt(III)/Pt(III) $[(C_6F_5)_2Pt(\mu\text{-}PPh_2)_2Pt(C_6F_5)_2]$(*Pt-Pt*) species, while reaction of $[NBu_4][(C_6F_5)_2Pt(\mu\text{-}PPh_2)_2M(acac)]$ (acac =

acetylacetonato, M = Pt, Pd) [17] with $[Ag(OClO_3)(PPh_3)]$ gave the silver adduct $[NBu_4][(C_6F_5)_2Pt(\mu\text{-}AgPPh_3)(\mu\text{-}PPh_2)_2M(acac)]$ (M = Pt, Pd) (Scheme 1). The related silver adduct $[(C_6F_5)_2Pt(\mu\text{-}AgOClO_3)(\mu\text{-}PPh_2)_2Pt(phen)]$ (phen = 1,10-phenantroline) was obtained from $[(C_6F_5)_2Pt(\mu\text{-}PPh_2)_2Pt(phen)]$ and $AgClO_4$. Complexes where the silver atom bridges Pd–P or Pt–P bonds were prepared starting from $[(C_6F_5)_2Pt(\mu\text{-}PPh_2)_2M(PPh_3)_2]$ and $AgClO_4$ (M = Pd, Pt) [18] or from $[(PHCy_2)Pt(\mu\text{-}PCy_2)\{\kappa^2\textit{P,O}\text{-}\mu\text{-}P(O)Cy_2\}Pt(PHCy_2)]$(*Pt–Pt*) and Ag(OTf) [19]. On the other hand, when the dipalladium species $[(C_6F_5)_2Pd(\mu\text{-}PPh_2)_2Pd(acac)]$ was treated with $[Ag(OClO_3)(PPh_3)]$, the complex $[(C_6F_5)(PPh_3)Pd(\mu\text{-}PPh_2)_2Pd(acac)]$, deriving from ligand substitution, was obtained (Scheme 1).

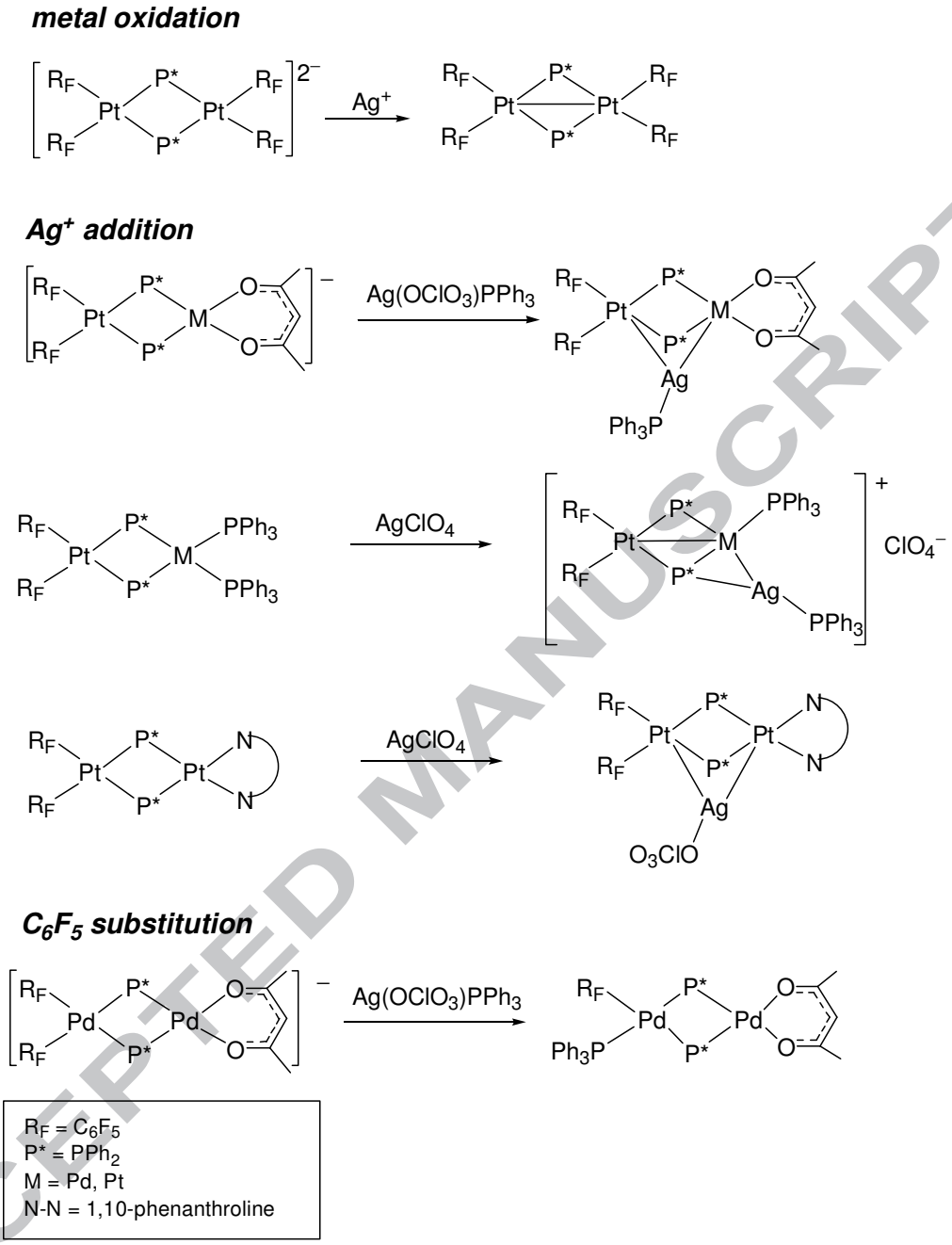

Scheme 1 Reactivity of phosphanido bridged dinuclear complexes towards Ag^+ electrophiles

As far as complexes with diphosphanes are concerned $[(C_6F_5)_2Pt(\mu\text{-}PPh_2)_2M(P\text{-}P)]$ [P-P = dppm, M = Pt (**A**), Pd (**B**); P-P = dppe, M = Pt (**C**), Pd (**D**)], their behavior towards Ag(I) depends not only on the type of phosphane used (dppm or dppe) but also on the metal centre M and on the electrophile reactant ($AgClO_4$ or $[Ag(OClO_3)(PPh_3)]$). An adduct with two Pt-Ag bonds is formed with the homonuclear Pt complex and dppm (**A**), while the heteronuclear derivative (Pt, Pd) gives a complex with the silver atom bridging the Pd–P bond (3c-2e$^-$ bond), see Scheme 2.

Complexes with dppe (**C**, **D**) react with $AgClO_4$ or $[Ag(OClO_3)(PPh_3)]$ in a rather different way, since a mirror of Ag^0 and $[(PPh_2C_6F_5)(C_6F_5)Pt(\mu\text{-}OH)(\mu\text{-}PPh_2)M(dppe)]ClO_4$ are formed. This result indicates that **C** or **D** are oxidized by Ag^+ to form the Pt/M (III) complex which in the presence of the nucleophile OH^- (moisture in the system) produces easily the PPh_2/C_6F_5 reductive coupling [12]. In no case complexes (**C**, **D**) facilitate insertion of the Ag^+ to form a 3c-2e$^-$ bond. It seems that in these Pt/Pd(II,II) complexes the insertion of silver into a M–P bond is only possible for M = Pd and dppm as chelating ligand. This fact could be related with the higher lability of the Pd–P bonds, when compared with the Pt–P ones, and with the higher tension of the four membered rings in complexes with dppm as compared with the five membered rings in complexes with dppe (see Scheme 2).

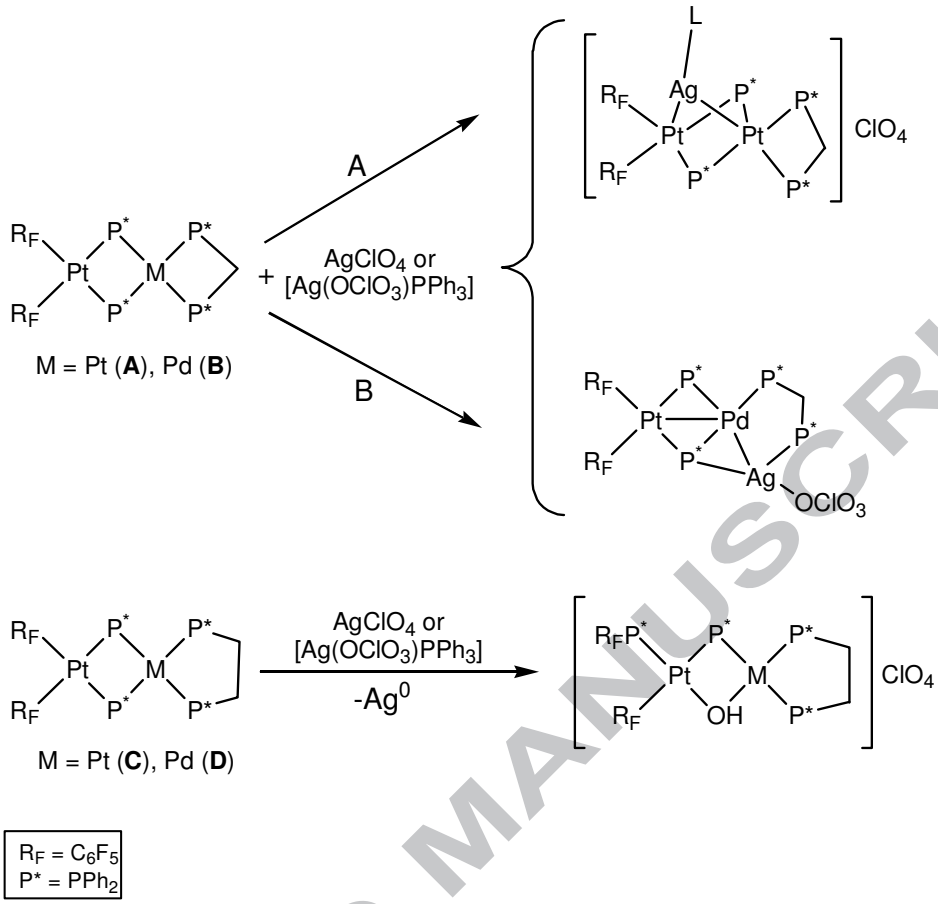

Scheme 2 Chemical behaviour of complexes **A-D** towards $AgClO_4$ or Ag $(OClO_3)$ PPh_3

Such a very different behaviour of the binuclear complexes (**A**, **B**, **C**, **D**) towards Ag^+ prompted us to complete the study by using homo- and heteronuclear Pt/Pd complexes with a different, more flexible, and easy to oxidize diphosphane: 1,1'-bis(diphenylphosphino)ferrocene [20-26].

In this paper we report the synthesis of the saturated trinuclear complexes $[(C_6F_5)_2Pt(\mu\text{-}PPh_2)_2M(dppf)]$, [dppf = 1,1'-bis(diphenylphosphino)ferrocene, M = Pt (**1**), Pd (**2**)], and their reactions towards silver species which resulted, in the case of **1**, in the substitution of PPh_3 for C_6F_5 and, in the case of **2**, in the insertion of the Ag atom into the Pd–P bond.

RESULTS AND DISCUSSION

Synthesis of $[(C_6F_5)_2Pt(\mu\text{-}PPh_2)_2M(dppf)]$ [dppf = 1,1'-bis(diphenylphosphino) ferrocene, M = Pt (1), Pd (2)]

The trinuclear complexes **1** and **2** were prepared by reaction of thf solutions of the *cis*-$[(C_6F_5)_2Pt(PPh_2)_2]^{2-}$ dianion (prepared *in situ* by treatment of *cis*-$[(R_F)_2Pt(PPh_2H)_2]$ with *n*-LiBu) with *cis*-MCl_2(dppf) (M = Pt, Pd) in 1:1 molar ratio (Scheme 3). The Pt/Pt/Fe complex **1** could also be prepared by reaction of $[(C_6F_5)_2Pt(\mu\text{-}PPh_2)_2Pt(NCMe)_2]$ [27] with 1,1'-bis(diphenylphosphino)ferrocene (1:1 molar ratio), while the Pt/Pd/Fe complex **2** could also be synthesized by reaction of the tetranuclear complex $[NBu_4]_2[(C_6F_5)_2Pt(\mu\text{-}PPh_2)_2Pd(\mu\text{-}Cl)_2Pd(\mu\text{-}PPh_2)_2Pt(C_6F_5)_2]$ [28] with dppf (1:2 molar ratio, Scheme 3).

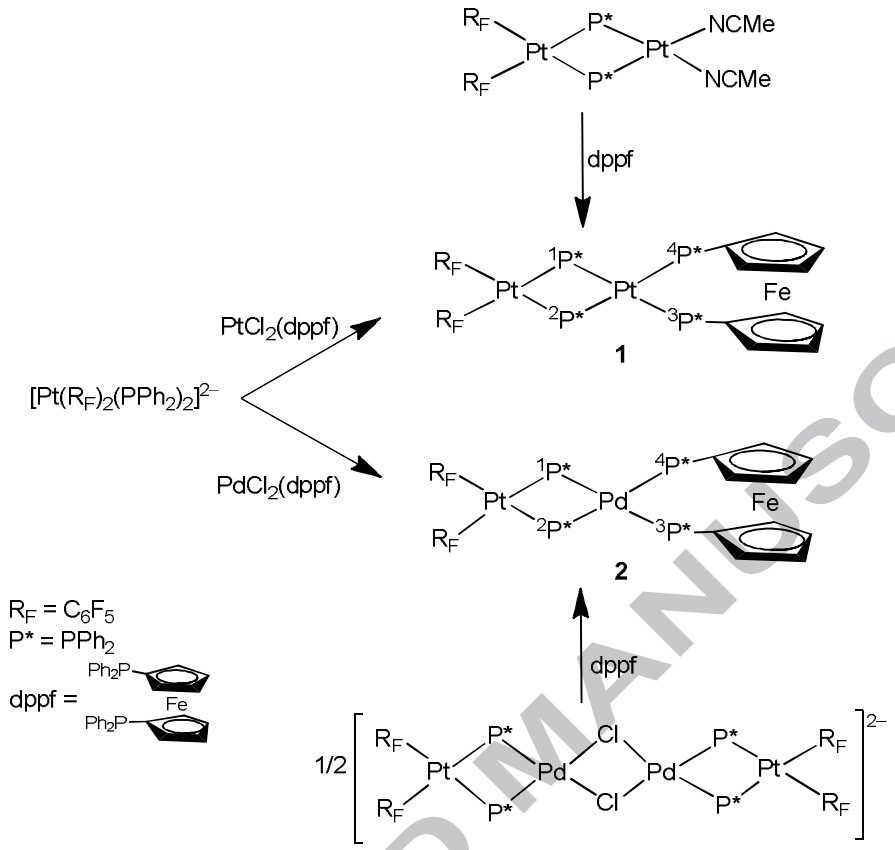

Scheme 3. Synthesis of trimetallic complexes **1** and **2**.

The IR spectra of **1** and **2** showed two absorptions in the 800 cm^{-1} region, in agreement with the presence of the *cis*-$Pt(C_6F_5)_2$ fragment [29, 30] and one absorption at 821 cm^{-1} due to the presence of the dppf ligand.

The $^{31}P\{^1H\}$ NMR spectra of **1** and **2** showed the pattern arising from superimposition of AA'XX', AA'XX'M and AA'XX'MM' spin systems (the latter only in the case of **1**) with A and X = ^{31}P and M = ^{195}Pt. The complexes showed two multiplets centred at δ –98.6 and δ 12.0 (for **1**, Figure 1) and at δ –98.2 and δ 13.6 (for **2**, Figure S2), flanked by appropriate ^{195}Pt satellites. The low-field signals (δ 12.0 for **1** and δ 13.6 for **2**) are ascribable to the P atoms of the dppf ligand chelate to Pt or Pd,

whereas the high-field signals (δ −98.6 for **1** and δ −98.2 for **2**) are in the range expected for bridging PPh_2 groups involved in four-membered P_2M_2 rings [12, 15, 17, 28, 31-36].

The $^{31}P\{^1H\}$ NMR signals of **1** and **2** were quite broad at 295 K and became even broader on lowering the temperature down to 253 K (Figure 1). Further lowering of the temperature down to 200 K produced, in the case of **2**, a $^{31}P\{^1H\}$ NMR spectrum consisting of three broad doublets (1:2:1 intensity ratio) in the phosphane region and two very broad doublets (3:1 intensity ratio), with platinum satellites, in the bridging phosphanide region (Figure 1). This behavior can be explained in terms of an equilibrium involving two synclinal staggered and the synperiplanar conformers of **2** deriving from torsion of the Cp rings [37] (Scheme 4).

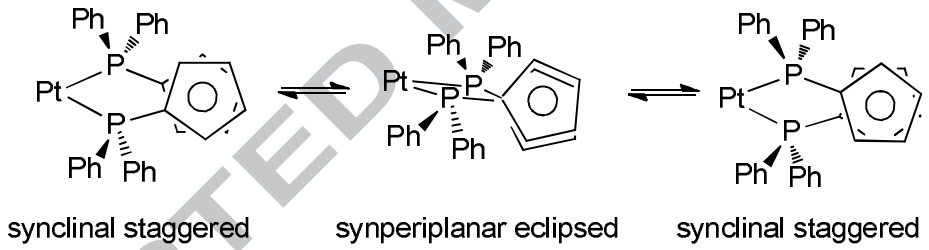

Scheme 4. Conformational equilibrium for **2**.

At temperatures equal or higher than 295 K the equilibrium is fast and the resulting $^{31}P\{^1H\}$ spectrum shows the averaged signals which become expectedly sharper on increasing the temperature up to 315 K (Figure 1). At low temperature the equilibrium is slowed down and at 200 K the molecules are "frozen" in one of the possible conformers (not necessarily the ideal ones depicted in Scheme 4, but also structures intermediate between the synclinal staggered and the synperiplanar eclipsed). The presence of several stable "frozen" conformers might rationalize the appearance of

more than two signals in the dppf region and of the 1:3 very broad doublets in the μ-PPh_2 region.

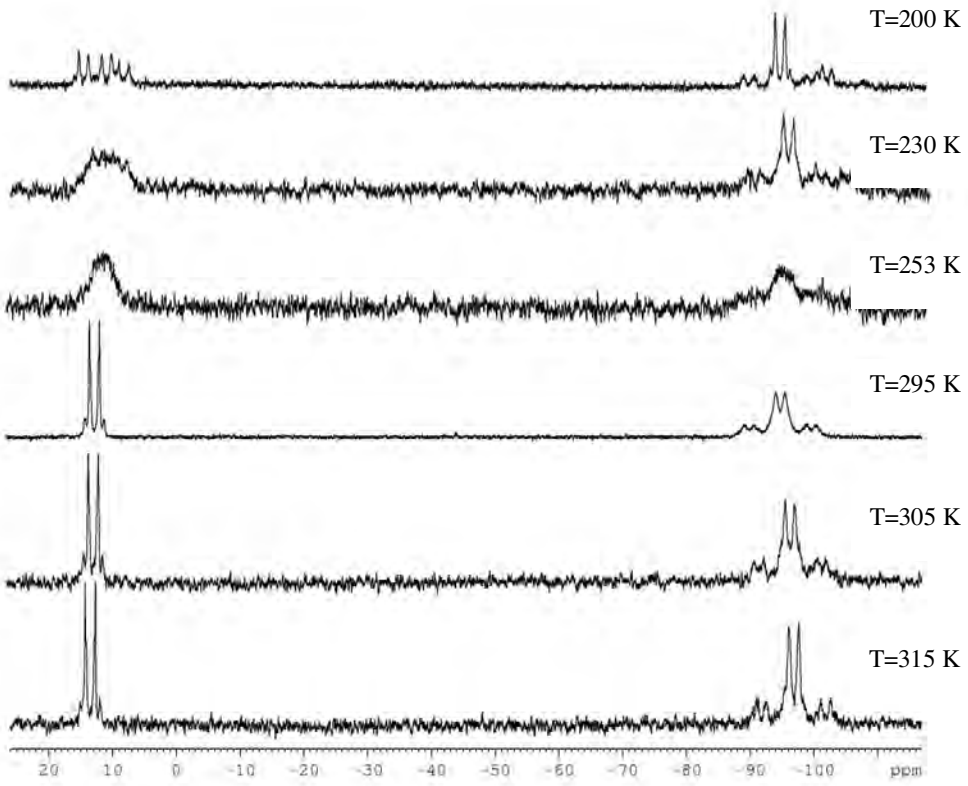

Figure 1. VT $^{31}P\{^1H\}$ NMR spectra of **2** (thf-d_8).

The ^{19}F NMR spectra of **1** and **2** at 298 K showed three signals in 2:2:1 intensity ratio due to the *o*-F, *m*-F, *p*-F atoms of the pentafluorophenyl rings, respectively. This pattern is in agreement with the presence of equivalent C_6F_5 groups. The *o*-F signals (δ –115.2 in **1** and δ –116.7 in **2**) as well as the *m*-F signals (δ –168.8 in **1** and δ –166.2 in **2**) are quite broad at 298 K, with platinum satellites overlapped to the central lines. The value of the coupling constant between the *o*-F and ^{195}Pt ($^3J_{F,Pt}$ = 325 Hz for **1** and **2**) was obtained by recording the ^{19}F NMR spectrum at 315 K, a temperature at which the signals became significantly sharper. The broadness of the ^{19}F signals observed at 298 K can be explained with the conformational equilibrium discussed above and/or with a

hindered rotation of the pentafluorophenyl rings about the Pt–C bond. That the conformational equilibrium determines, at least in part, the broadness of the ^{19}F NMR signals at 298 K seems confirmed by the ^{19}F NMR spectrum of **2** at 200 K, which showed six broad signals of different intensity in the *o*-F region. If only hindered rotation of the pentafluorophenyl rings about the Pt-C bond were responsible for the broadness of the ^{19}F NMR signals at 298 K, then a maximum of four *o*-F signals could be expected.

For all complexes described in this paper, the ^{195}Pt NMR signals of the pentafluorophenyl-bound Pt^1 atoms were detected by recording ^{19}F–^{195}Pt HMQC spectra exploiting the strong scalar coupling between the *ortho* fluorines and Pt, while the ^{195}Pt NMR signals belonging to the "Pt^2(dppf)" fragment were found by means of 1D ^{195}Pt{^{1}H} NMR experiments. Thus, the Pt^1 resonances for **1** (Figure 2a) and **2** (Figure 2b) were found as broad triplets at δ –3761 and δ –3610, respectively, while that of Pt^2 (in the case of **1**) was found as a multiplet at δ –4235.

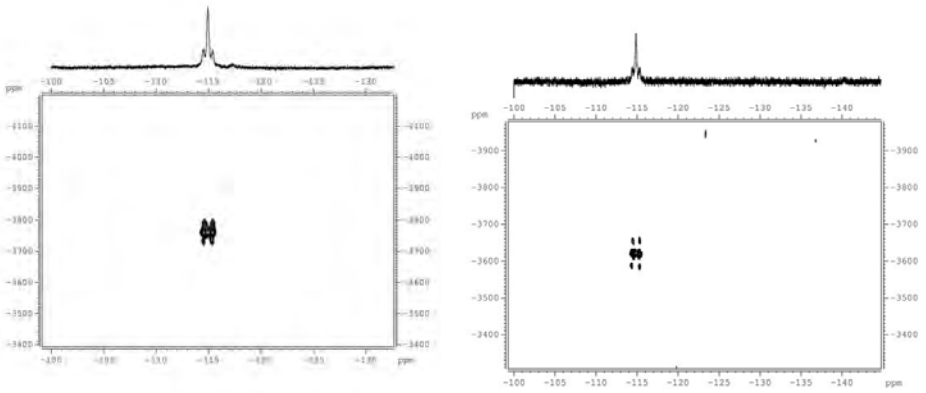

(a) (b)

Figure 2. ^{19}F–^{195}Pt HMQC NMR spectra of **1** (a) and **2** (b) (thf-d_8, 315 K).

Slow evaporation of the solvent from a dichloromethane solution of **2** afforded microcrystals that were submitted to XRD analysis. Although the crystals were not of sufficient quality to get a complete structure determination, it was possible to establish with certainty the atom connectivity. The complex **2** crystallizes with 1.5 molecules of CH_2Cl_2 per molecule of complex. Complex **2** is a trinuclear derivative (Figure S1), wherein two diphenylphosphanide ligands are acting as a bridge between the metal centres. The coordination sphere of the platinum centre is completed with two terminal pentafluorophenyl ligands and that of the palladium atom with the dppf ligand. The environments of the platinum and palladium atoms are square-planar, and the long Pd···Pt distance (3.4 Å) is indicative of the absence of a metal-metal bond. The ligand dppf chelate adopts the synclinal staggered conformation.

Reactivity of the Pt/Pt/Fe complex 1 towards $Ag(OClO_3)(PPh_3)$] and I_2

The reaction of $[Ag(OClO_3)(PPh_3)]$ with **1** (2:1 molar ratio) in CH_2Cl_2 at room temperature afforded, after work-up, a yellow solid identified as $[(PPh_3)(C_6F_5)Pt(\mu\text{-}PPh_2)_2Pt(dppf)][ClO_4]$ (**3**), in which the triphenylphosphane replaced a C_6F_5 group (Scheme 5). During the reaction no Ag metal was observed, suggesting that Ag^+ extracts one of the C_6F_5 groups to form, probably, AgC_6F_5 and transferring PPh_3 onto Pt. This Ag^+ promoted ligand exchange process is not unprecedented, being already observed in other platinum and palladium complexes [38, 39].

When $AgClO_4$ was used instead of $[Ag(OClO_3)(PPh_3)]$ in the reaction with **1**, Ag metal immediately formed but only a mixture of uncharacterizable species could be isolated from the reaction mixture. In order to try to oxidize the diplatinum complex **1** with a milder oxidant than $AgClO_4$, we carried out the reaction of **1** with I_2 that, however, afforded smoothly the complex $[(C_6F_5)(I)Pt(\mu\text{-}PPh_2)_2Pt(dppf)]$ (**4**) in which a iodide replaced a C_6F_5 group (Scheme 5). Although it is conceivable that the reaction

takes place through the oxidative addition of I_2 to **1**, with formation of a mixed valence Pt(IV)/Pt(II)/Fe(II) intermediate of formula $[(C_6F_5)_2Pt(I)_2(\mu\text{-}PPh_2)_2Pt(dppf)]$ [14, 35], our attempts to detect such intermediate were unsuccessful.

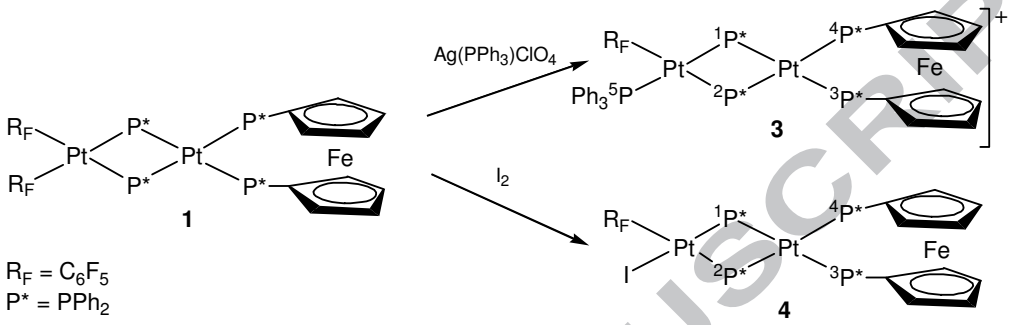

Scheme 5. Reactivity of **1** with $[Ag(OClO_3)(PPh_3)]$ and I_2.

Slow diffusion of *n*-hexane into CH_2Cl_2 solutions of **3** or **4** afforded crystals suitable for XRD studies. Complex **3** crystallizes with half a molecule of dichloromethane. In the cation $[(C_6F_5)(PPh_3)Pt(\mu\text{-}PPh_2)_2Pt(dppf)]^+$ (Figure 3) two diphenylphosphanide ligands are acting as a bridge between the metal centres. Each platinum atom is located in a square-planar environment formed, in addition to the diphenylphosphanide ligands, by the C_6F_5 and PPh_3 ligands in the case of Pt(1) and the ligand dppf in the case of Pt(2). The environments of the centres are not coplanar, the dihedral angles between the Pt planes being 159.8(1) º. The large distance between the two metal centres Pt(1)···Pt(2), 3.646(1) Å, is indicative of the absence of metal-metal bond, as expected for complexes with 32 valence electrons in the skeleton [40]. The values of the P–Pt–P and Pt–P–Pt angles (Table 1) are of the order of magnitude expected for this type of systems.

As for complex **2**, in complex **3** the dppf adopt a synclinal staggered conformation, with torsion angle between the Cp rings of 36.47 º and with the angle formed by the Cp ring planes of 4.84 º.

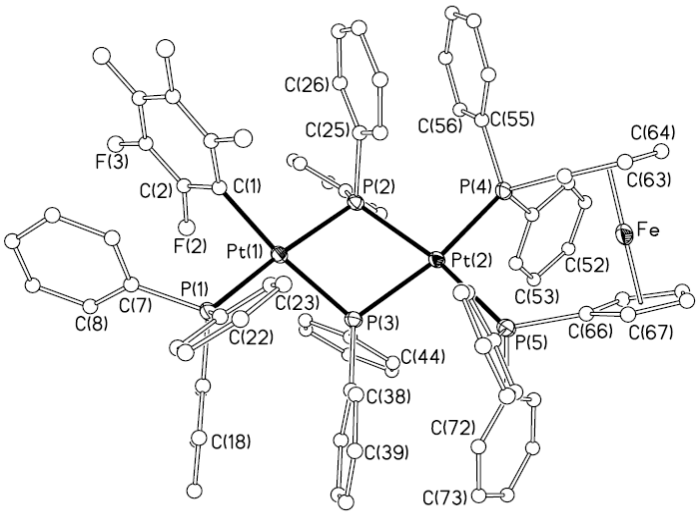

Figure 3. Structure of the cation in complex $[(PPh_3)(C_6F_5)Pt(\mu\text{-}PPh_2)_2Pt(dppf)][ClO_4]\cdot 0.5CH_2Cl_2$ (**3**$\cdot 0.5CH_2Cl_2$).

Table 1. Selected bond distances (Å) and angles (°) for $[(PPh_3)(C_6F_5)Pt(\mu\text{-}PPh_2)_2Pt(dppf)][ClO_4]\cdot 0.5CH_2Cl_2$ (**3**$\cdot 0.5CH_2Cl_2$).

	Distances (Å)		
Pt(1)–C(1)	2.069(7)	Pt(2)–P(4)	2.3495(18)
Pt(1)–P(1)	2.3106(18)	Pt(2)–P(2)	2.3596(18)
Pt(1)–P(3)	2.3130(18)	Pt(2)–P(5)	2.3733(18)
Pt(1)–P(2)	2.3249(18)	Pt(2)–P(3)	2.3824(18)
	Angles (°)		
C(1)–Pt(1)–P(1)	89.84(18)	P(4)–Pt(2)–P(2)	95.22(6)
C(1)–Pt(1)–P(3)	166.63(19)	P(4)–Pt(2)–P(5)	96.43(6)
C(1)–Pt(1)–P(2)	94.90(18)	P(2)–Pt(2)–P(5)	165.71(7)
P(1)–Pt(1)–P(3)	101.75(6)	P(4)–Pt(2)–P(3)	163.80(6)
P(1)–Pt(1)–P(2)	171.37(6)	P(2)–Pt(2)–P(3)	72.60(6)
P(3)–Pt(1)–P(2)	74.50(6)	P(5)–Pt(2)–P(3)	97.31(6)
Pt(1)-P(2)-Pt(2)	102.22(6)	Pt(1)-P(3)-Pt(2)	101.88(7)

Complex **4** crystallizes with two molecules of CH_2Cl_2 per molecule of complex (Figure 4). $[(C_6F_5)IPt(\mu\text{-}PPh_2)_2Pt(dppf)]$ contains two platinum atoms, both located in distorted square planar environments connected by two bridging diphenylphosphanido ligands. As can be seen from the values of distances and angles (Table 2), the Pt(2) environment has a greater distortion than that corresponding to the Pt(1) one, probably due to steric restriction of the ligand dppf. On the other hand, the distances Pt–P are slightly shorter in the case of Pt(1) than in the case of Pt(2). The dihedral angle between the Pt planes is 132.9(1) º. The Pt(1)···Pt(2) distance (3.466(1) Å), is indicative of the absence of Pt–Pt bond, (32 VEC) [40].

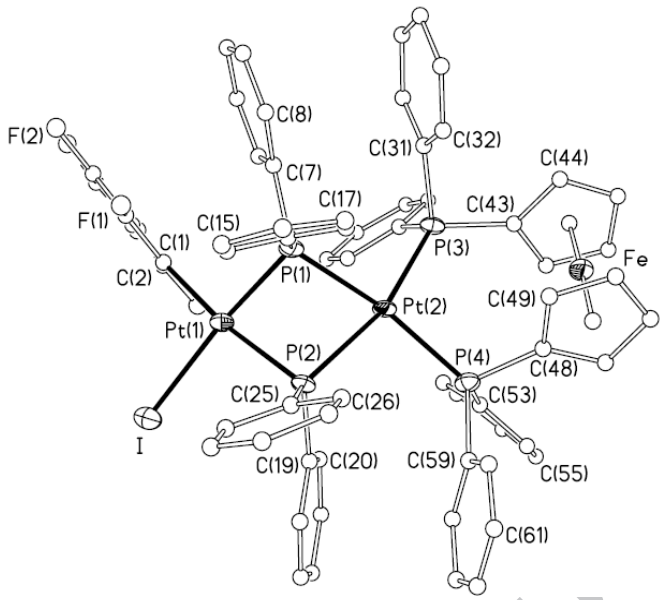

Figure 4. Molecular structure of the complex $[(C_6F_5)(I)Pt(\mu\text{-}PPh_2)_2Pt(dppf)]\cdot 2CH_2Cl_2$ (**4**$\cdot 2CH_2Cl_2$).

In **4,** the dppf adopt a synclinal staggered conformation, with torsion angle between the Cp rings of 40.08 º and with the angle formed by the Cp ring planes of 3.96º.

Table 2. Selected bond distances (Å) and angles (°) for $[(C_6F_5)(I)Pt(\mu–PPh_2)_2Pt(dppf)]\cdot 2CH_2Cl_2$ (**4**$\cdot 2CH_2Cl_2$).

Distances (Å)

Pt(1)–C(1)	2.080(14)	Pt(2)–P(4)	2.338(4)
Pt(1)–P(1)	2.258(4)	Pt(2)–P(3)	2.355(3)
Pt(1)–P(2)	2.321(4)	Pt(2)–P(1)	2.364(4)
Pt(1)–I	2.6698(11)	Pt(2)–P(2)	2.372(3)

Angles (°)

C(1)–Pt(1)–P(1)	99.4(4)	P(4)–Pt(2)–P(3)	97.16(12)
C(1)–Pt(1)–P(2)	170.8(4)	P(4)–Pt(2)–P(1)	167.64(11)
P(1)–Pt(1)–P(2)	74.96(13)	P(3)–Pt(2)–P(1)	94.73(12)
C(1)–Pt(1)–I	88.6(4)	P(4)–Pt(2)–P(2)	97.38(12)
P(1)–Pt(1)–I	171.35(9)	P(3)–Pt(2)–P(2)	159.37(13)
P(2)–Pt(1)–I	97.57(9)	P(1)–Pt(2)–P(2)	72.07(12)
Pt(1)-P(1)-Pt(2)	97.06(14)	Pt(1)-P(2)-Pt(2)	95.13(12)

The IR spectra of **3** and **4** show one absorption at 782 or 780 cm^{-1}, respectively, in accord with the presence of one Pt-C_6F_5 group. A band at 623 cm^{-1}, ascribable to ClO_4^-, is also present in the IR spectrum of **3**.

The $^{31}P\{^1H\}$ NMR spectrum of **3** in acetone-d_6 at 295 K (Figure S3) is consistent with the structure found in the solid state and shows a doublet ascribable to the Pt bound PPh_3 at δ 19.9 ($^2J_{P,P}$ = 335 Hz, $^1J_{Pt(1),P(1)}$ = 2271 Hz), the doublets ascribable to the P atoms of the dppf at δ 16.5 ($^2J_{P,P}$ = 283 Hz, $^1J_{Pt,P}$ = 2162 Hz) and at δ 12.5 ($^2J_{P,P}$ = 289 Hz, $^1J_{Pt–P}$ = 2270 Hz) and two multiplets centred at δ –128.7 and δ –138.5 due to the P atoms of the two inequivalent μ-PPh_2 groups.

In the case of **4**, the $^{31}P\{^1H\}$ NMR spectrum showed two doublets at δ 15.1 (P^3) and at δ 12.3 (P^4) due to the inequivalent P atoms of the coordinated dppf, and a multiplet centred at δ –116.8 due to the P atoms of the two almost isochronous PPh_2 groups. The

$^{31}P\{^{1}H\}$ COSY spectrum of **4** (Figure 5) allowed us to determine unequivocally the ^{31}P-^{195}Pt coupling constants that were not directly extractable from the monodimensional $^{31}P\{^{1}H\}$ NMR spectrum because of overlapping of the ^{195}Pt satellites. It is noticeable the significant difference observed for the $^{1}J_{P(1),Pt(1)}$ comparing **3** (1874 Hz) with **4** (2713 Hz), as a consequence of the different *trans*-influence of PPh_3 and I [10, 12, 15, 18, 31, 41-44].

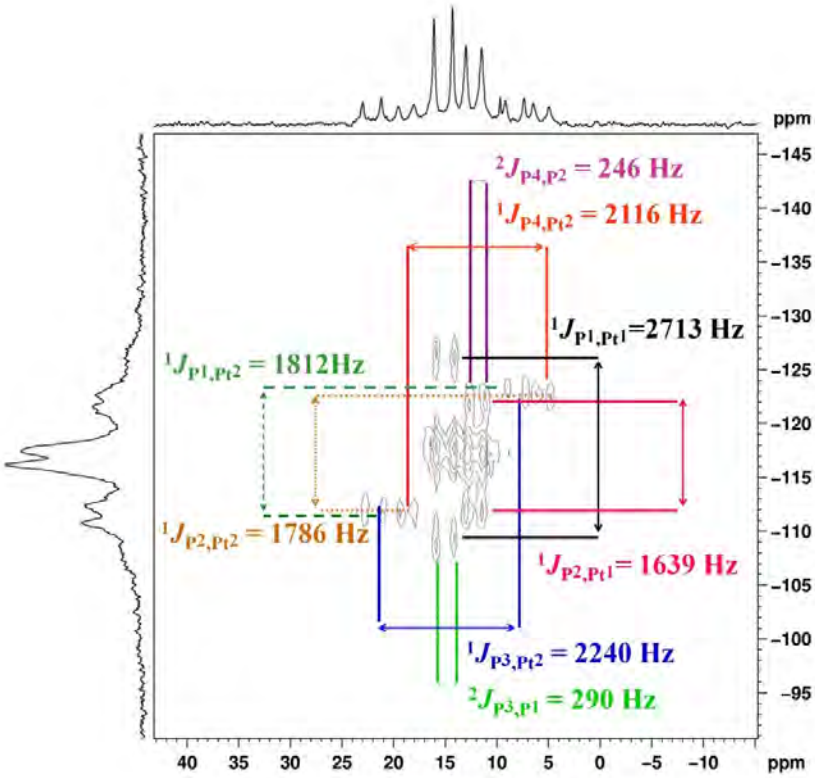

Figure 5. Portion of the $^{31}P\{^{1}H\}$ COSY spectrum of **4** (CD_2Cl_2, 295 K).

The ^{19}F NMR spectra in acetone-d_6 of **3** and **4** at room temperature showed three signals for the *o*-F, *p*-F, and *m*-F atoms of the pentafluorophenyl ring. The *o*-F signals (δ –116.2 for **3**, δ –116.0 for **4**) are flanked by platinum satellites from which the coupling constants $^{3}J_{Pt(1),F}$ = 237 Hz (**3**) and $^{3}J_{Pt(1),F}$ = 296 Hz (**4**) could be directly extracted.

The ^{195}Pt signal of the pentafluorophenyl bonded Pt^1 was found at δ –4069 for **3** and at δ –3930 for **4**, while the Pt^2 signal was found at δ –4238 for **3** and at δ –4298 for **4**.

Reactivity of the Pt/Pd/Fe complex 2 towards $AgClO_4$

The addition of $AgClO_4$ to a dichloromethane solution of **2** at room temperature afforded the adduct $[(R_F)_2Pt(\mu\text{-}PPh_2)_2Pd(dppf)Ag][ClO_4]$ (**5**) featuring a Pd–Ag bond (Scheme 6). The same adduct was formed when **2** was treated with $[Ag(OClO_3)(PPh_3)]$, although in this reaction, complex **5** was obtained in mixture with $[Ag(PPh_3)_2][ClO_4]$.

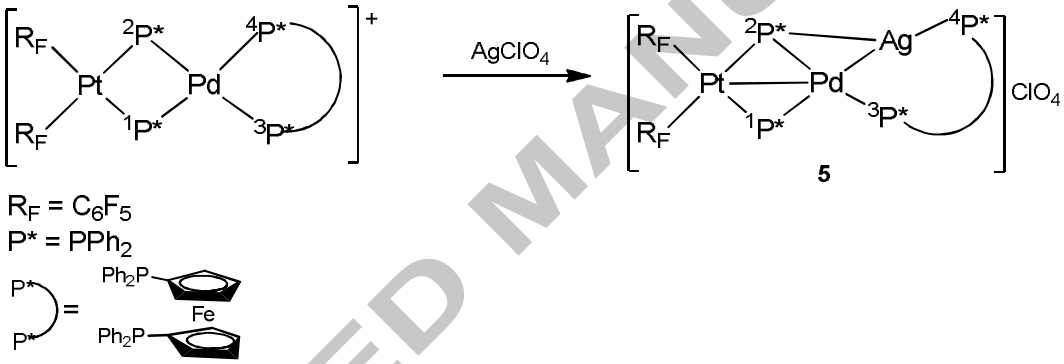

Scheme 6. Reactivity of **2** with $AgClO_4$.

The crystal structure of **5** is depicted in Figure 6, with relevant bond distances and angles collected in Table 3.

Complex **5** is a tetranuclear compound containing platinum, palladium, iron(II) and silver(I). As can be seen, complex **5** is the result of the insertion of Ag^+ into a Pd–P (of the dppf) bond of complex **2**.

Due to this insertion, Ag^+ is bonded to P(4), Ag–P(4) = 2.385(2) Å, and to the Pd–P(2) bond (3c-2e$^-$) forming Pd–Ag and Ag–P(2) bonds [Ag–P(2) = 2.513 (2), Pd–Ag = 2.6863 (8) Å].

Finally, the Pt–Pd distance is short, 2.7002(6) Å, and indicates the existence of a Pt–Pd bond, as expected for a complex with 30 VEC [10, 12, 15, 18, 31, 41-44].

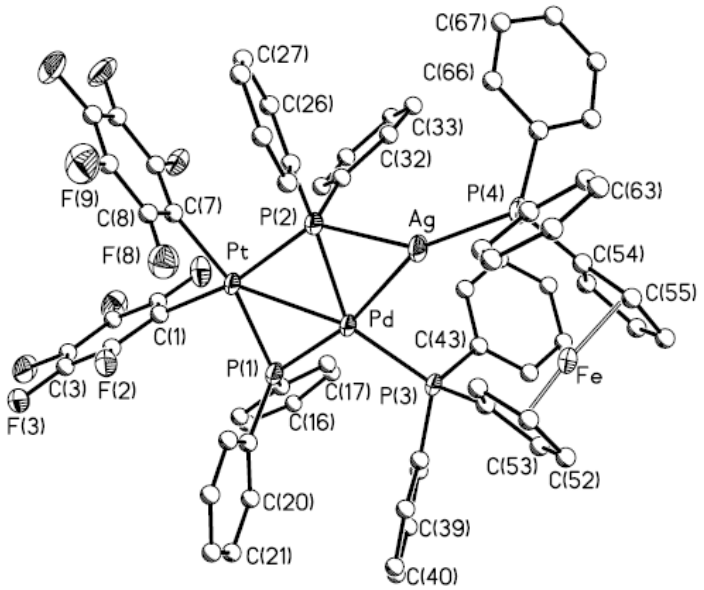

Figure 6. Structure of the cation in the complex **5**·CH_2Cl_2·*n*-hexane.

The Pt coordination environment is conventional, while the Pd centre displays a distorted, square planar coordination plane, probably due to the special Pd–Ag bond.

In complex **5** the dppf adopt an eclipsed conformation (torsion angle between the Cp rings 1.09 º), with the C*ipso* atoms not eclipsating each other but the adjacent C atom. The angle formed by the Cp ring planes is 4.12 º.

Table 3. Selected bond distances (Å) and angles (°) for $[(C_6F_5)_2Pt(\mu–PPh_2)_2Pd(dppf)Ag][ClO_4]\cdot CH_2Cl_2\cdot$*n*-hexane (**5**$\cdot CH_2Cl_2\cdot$*n*-hexane).

Distances (Å)

Pt–C(1)	2.073(7)	Ag–P(4)	2.385(2)
Pt–C(7)	2.081(7)	Ag–Pd	2.6863(8)
Pt–P(1)	2.2851(19)	Pd–P(1)	2.220(2)
Pt–P(2)	2.3502(19)	Pd–P(3)	2.291(2)
Pt–Pd	2.7002(6)	Pd–P(2)	2.348(2)
Ag–P(2)	2.513(2)		

Angles (°)

C(1)–Pt–C(7)	86.4(3)	P(2)–Pt–Pd	54.88(5)
C(1)–Pt–P(1)	83.42(19)	P(4)–Ag–P(2)	148.99(7)
C(7)–Pt–P(1)	165.9(2)	P(1)–Pd–Ag	165.94(6)
C(1)–Pt–P(2)	164.6(2)	P(3)–Pd–Ag	89.08(5)
C(7)–Pt–P(2)	85.8(2)	P(2)–Pd–Ag	59.44(5)
P(1)–Pt–P(2)	106.33(7)	P(1)–Pd–P(3)	104.52(7)
Ag–Pd–Pt	112.48(2)	P(1)–Pd –P(2)	108.60 (7)
C(1)–Pt–Pd	135.38(18)	P(3)–Pd–P(2)	143.63(7)
C(7)–Pt–Pd	137.9(2)	P(2)–Ag–Pd	53.56(5)
P(1)–Pt–Pd	52.07(5)	P(4)–Ag–Pd	154.09(5)

The formation of complex **5** can be explained by the insertion of the atom of silver in the Pd–P(4) (phosphorus atom of the dppf) bond with formation of Pd–Ag and Ag–(μ-P) bonds. The electronic requirements of the palladium centre are satisfied with the formation of a Pt–Pd bond and those of silver with an interaction with the phosphorus atom of the diphenylphosphanide bridge. In fact, the Pd–(μ-PPh_2) bond acts as donor of electrons towards the silver atom with formation of a system of three centres–two electrons (3c, $2e^-$) Ph_2P–Ag–Pd. This coordination of P(2) implies that the group diphenylphosphanide is a binder between three metal centres. Similar examples exists in

the literature, such as $[(C_6F_5)_2Pt(\mu\text{-}PPh_2)_2Pd(dppm)Ag(PPh_3)(ClO_4)]$ [12] and $[(PPh_3)Au(PPh_3)Pt(\mu\text{-}PPh_2)_2Pt(PPh_3)Au(PPh_3)]^{2+}$ [45].

The NMR features of **5** indicate that the structure observed in the solid state is maintained in solution at low temperature, and that at 295 K the complex undergoes a fluxional process during which the Ag atom binds alternatively each of the two bridging phosphanides.

The $^{31}P\{^1H\}$ NMR spectrum of **5** at 200 K (Figure 7) shows four signals centred at δ 298.4, δ 144.3, δ 25.9 and δ 9.4. Of these, the lowfield signals at δ 298.4 and δ 144.3 can be assigned to the bridging phosphanides subtending a Pt–Pd bond [36]. In particular, the signal at δ 298.4 can be assigned to the phosphanido P^1 bridging two metal centres, μ^2-PPh_2, while that at δ 144.3 has to be ascribed to the phosphanido P^2 bridging three metal centres, μ^3-PPh_2. A similar difference in the value of the ^{31}P chemical shift on going from a μ^2-PPh_2 to a μ^3-PPh_2 coordination mode (for **5**: $\Delta\delta$ = 154.1 ppm) has been observed before for the complex $[AgPdPt(\mu\text{-}PPh_2)_2(R_F)_2(OClO_3)(dppm)]$ ($\Delta\delta$ = 154.9 ppm) [12]. The signals at δ 25.9 and δ 9.4 are ascribable to the dppf P^3 and P^4 atoms, respectively. The presence of the Pt–Pd bond is supported by the value of the coupling between Pt and P^3 atoms, $^2J_{Pt,P(3)}$ = 130 Hz. The signals of P^4 and P^1 show the couplings with ^{109}Ag ($J_{P(4),109Ag}$ = 551 Hz; $J_{P(1),109Ag}$ = 250 Hz) and with ^{107}Ag ($J_{P(4),109Ag}$ = 479 Hz; $J_{P(1),109Ag}$ = 250 Hz).

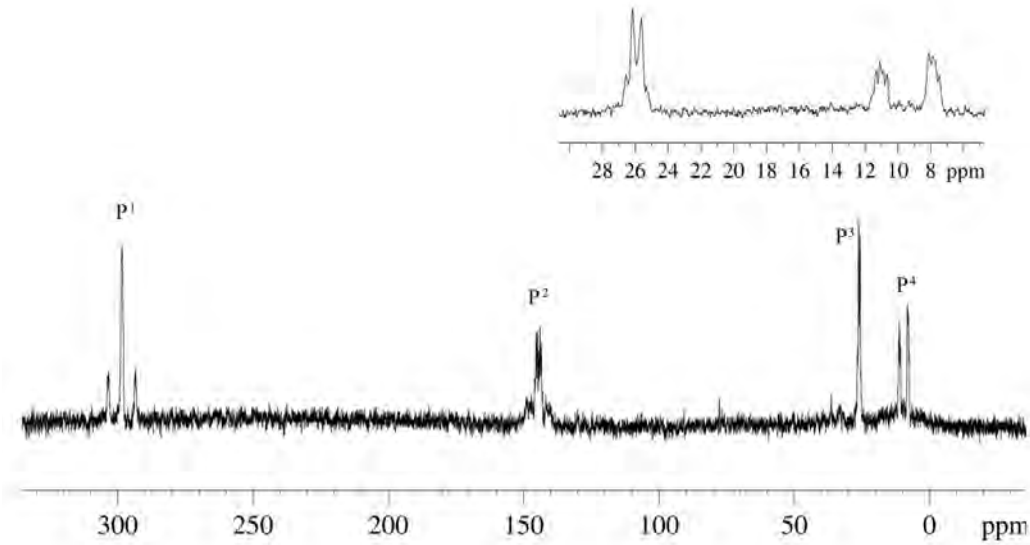

Figure 7. $^{31}P\{^{1}H\}$ NMR spectrum of **5** (acetone-d_6, 200 K).

The ^{19}F NMR spectrum of **5** at 200 K showed, at low fields, three signals for the *ortho*-F atoms in a 1:1:2 ratio, indicating the presence of one C_6F_5 ring ($\delta_{o\text{-}F}$ –115.8 and $\delta_{o\text{-}F}$ –117.9) rotating more slowly than the other ($\delta_{o\text{-}F}$ –119.6).

On increasing the temperature from 200 K to 295 K resulted in a progressive broadening of the $^{31}P\{^{1}H\}$ NMR signals of the bridging phosphanides P^1 and P^2 which is indicative of a dynamic process involving the tetranuclear complex **5**.

In order to gain insights into the dynamic process occurring for **5**, we recorded a $^{31}P\{^{1}H\}$ EXSY spectrum at 273 K (Figure 7) which showed cross peaks between P^2 and P^1 signals but not between P^4 and P^3. This outcome can be explained admitting that the Pd–Ag and P^2–Ag bonds are constantly broken and reformed, while the Pd and P^3 atoms remain bonded to each other (Scheme 7). The mechanism envisages the breaking and reforming of the weakest bonds in the molecule, and it parallels the mechanism validated for the dynamic process occurring for [AgPdPt(μ-$PPh_2)_2(C_6F_5)_2(OClO_3)$(dppm)] in solution [12].

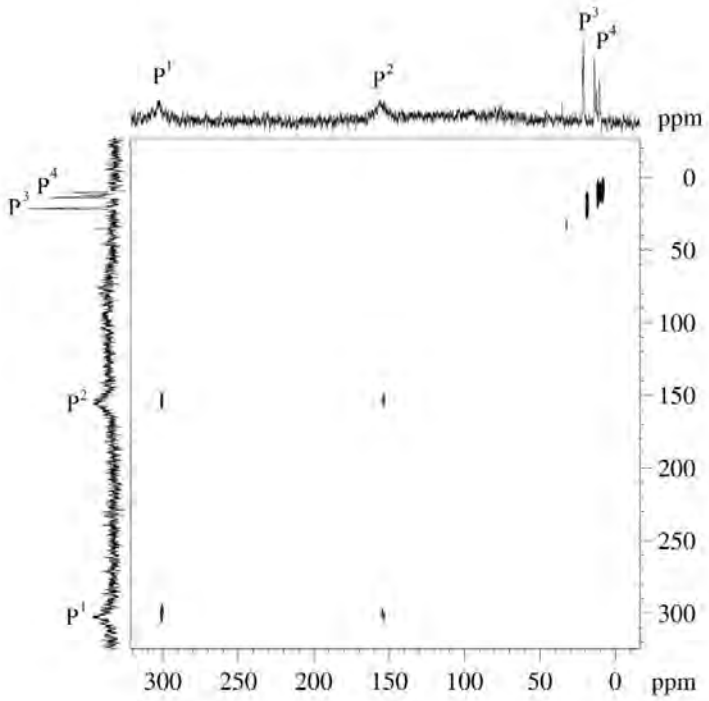

Figure 8. $^{31}P\{^{1}H\}$ EXSY spectrum of **5** (acetone-d_6, 273 K).

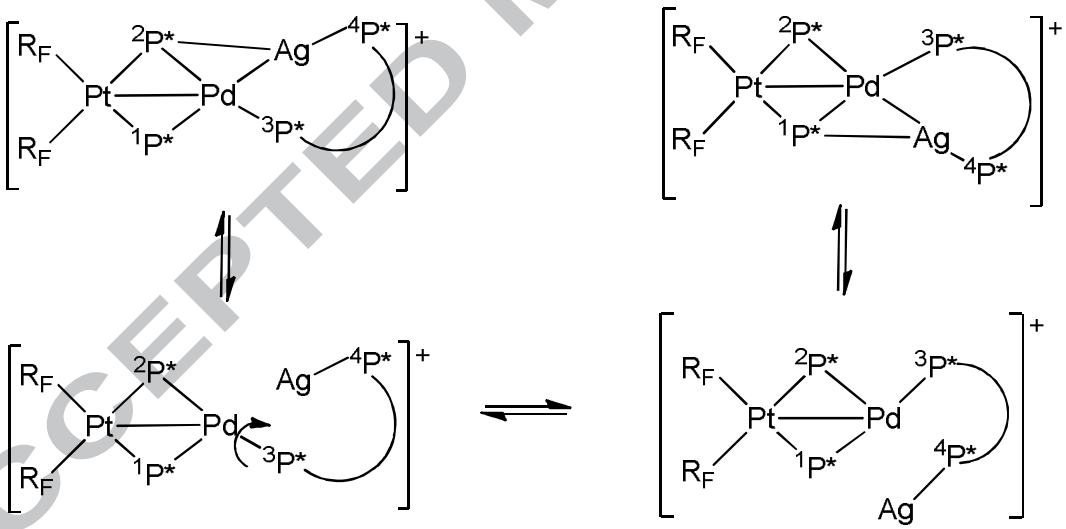

Scheme 7. The dynamic process occurring for **5** in solution

CONCLUDING REMARKS

Phosphanido groups have shown to be excellent ligands in the development of molecular architecture and in the synthesis of specific transition metal complexes. The

dinuclear phosphanido complexes $[(R_F)_2Pt(\mu\text{-}PPh_2)_2M(dppf)]$ (M = Pt (**1**); M = Pd(**2**)) react with Ag^+, $Ag(PPh_3)^+$, in diferent ways depending on the nature of M. So, in no case such binuclear complexes act as metal- donor ligands towards Ag^+ or $Ag(PPh_3)^+$ a rather frequent behaviour in reactions of Pt(II) complexes with these Lewis acids. $[(R_F)_2Pt(\mu\text{-}PPh_2)_2Pd(dppf)]$ reacts either with Ag^+ or $Ag(PPh_3)^+$ producing an insertion of Ag^+ into the Pd-P bond and giving an uncommon tetranuclear with a system of three centres–two electrons ($3c,2e^-$) (Pd-P-Ag). The trinulear complex $[(R_F)_2Pt(\mu\text{-}PPh_2)_2Pt(dppf)]$ does not allow the insertion of the Ag^+ into the stronger and inert Pt-P bond when reacts either with $Ag(PPh_3)^+$ or Ag^+ and in both cases the Ag^+ acts as a C_6F_5 scavenger eliminating AgC_6F_5 and forming **3** (which contains PPh_3 bonded to platinum) when the reaction is carried out with $Ag(PPh_3)^+$ or producing a mixture of uncharacterizable species when the reaction is carried out with $AgClO_4$. As in other cases, the number of VEC of the skeleton (32 or 30) is related with the formation (**5**) or not (**1**-**4**) of Pt–M bonds.

EXPERIMENTAL SECTION

General Procedures and Materials. C, H analyses were performed with a Perkin Elmer 240B micro-analyzer. IR spectra were recorded on a Spectrum One FT-IR Spectrometer (Nujol mulls between polyethylene plates in the range 4000-200 cm^{-1}). NMR spectra were recorded with a Bruker Avance 400 Spectrometer with $SiMe_4$, $CFCl_3$, 85% H_3PO_4, and H_2PtCl_6 as external references for ^1H, ^{19}F, ^{31}P, and ^{195}Pt, respectively. Conductivity measurements were performed using the conductivity bridge model Philips PW 9509 on solutions of the acetone and dichloromethane, the concentration approximately 5×10^{-4} M.

Literature methods were used to prepare the starting materials 1,1'-bis(difenilfosfino)ferrocene (dppf) [46], $[M(dppf)Cl_2]$ [M = Pd; Pt] [47, 48],

$[(C_6F_5)_2Pt(\mu–PPh_2)_2Pt(NCCH_3)_2]$ [27], $[NBu_4]_2[(C_6F_5)_2Pt(\mu\text{-}PPh_2)_2Pd(\mu\text{-}Cl)_2Pd(\mu\text{-}PPh_2)_2Pt(C_6F_5)_2]$ [28] and *cis*-$[(C_6F_5)_2Pt(PPh_2H)_2]$ [28].

Caution! *Perchlorate salts of metal complexes with organic ligands are potentially explosive. Only small amounts of material should be prepared, and these should be handled with great caution.*

Synthesis of $[(C_6F_5)_2Pt(\mu\text{-}PPh_2)_2Pt(dppf)]$ (1)

Method a. *n*-LiBu (0.45 mL of a 2.47 M *n*-hexane solution, 1.11 mmol) was added under an argon atmosphere to a colourless solution of *cis*-$[(C_6F_5)_2Pt(PPh_2H)_2]$ (0.500 g, 0.554 mmol) in thf (30 ml) at 195 K. The yellow solution was stirred for 20 min, and then $[Pt(dppf)Cl_2]$ (0.454 g, 0.554 mmol) was added and allowed to react at room temperature for 12 h. The resulting suspension was evaporated to dryness. CH_2Cl_2 (40 mL) was added to the residue. The mixture was filtered through celite, and the resulting solution evaporated to *ca*. 1 mL produced a yellow precipitate of **1**, which was filtered off and washed with Et_2O (2 × 2mL). Yield: 0.437 g, 50%.

Method b. To a colorless solution of $[(C_6F_5)_2Pt(\mu\text{-}PPh_2)_2Pt(NCMe)_2]$ (0.150 g, 0.127 mmol) in acetone (5 mL) was added dppf (0.071 g, 0.127 mmol). The resulting yellow solution was stirred at room temperature for 1 h and then evaporated to 2 mL. Complex **1** crystallized as a yellow solid, which was filtered, washed with Et_2O (2 × 2 mL) and vacuum-dried. Yield: 0.178 g, 85%.

Anal. Found (Calcd for $C_{70}H_{48}F_{10}FeP_4Pt_2$): C, 51.07 (50.99); H, 3.08 (2.93). IR (Nujol, cm^{-1}): 1161 (vs), 821 (s) dppf; 952 (vs), 781(vs) (Fermi res., C_6F_5), 772 (vs) (X-sensitive C_6F_5). ^1H NMR (thf-d_8, 295 K, 400 MHz): δ 4.10 (s, $C_\beta H$, 4 H), 4.41 (s, $C_\gamma H$, 4 H), from 6.5 to 8.5 (m, *Ph*, 40 H). ^{19}F NMR (thf-d_8, 300 K, 376.5 MHz): δ –116.7 (4 *o*-F, $^3J_{F,Pt(1)}$ = 325 Hz), –168.8 (m, 4 *m*-F), –169.6 (t, 2 *p*-F, $^3J_{F,F}$ = 20 Hz); $^{31}P\{^1H\}$

NMR (thf-d_8, 295 K, 162 MHz): δ 12.0 (m, $^2J_{P(3),P(1)} = {}^2J_{P(4),P(2)}$ = 239 Hz, $^2J_{P(3),P(4)}$ = 55 Hz, $^2J_{P(3),P(2)} = {}^2J_{P(4),P(1)}$ = 14 Hz, $^1J_{P,Pt}$ =2210 Hz, $P^{3/4}$), –98.6 (m, $^2J_{P(1),P(3)} = {}^2J_{P(2),P(4)}$ = 239 Hz, $^2J_{P(1),P(2)}$ = 111 Hz, $^2J_{P(1),P(4)} = {}^2J_{P(2),P(3)}$ = 14 Hz, $^1J_{P,Pt(1)}$ = 1802 Hz, $^1J_{P,Pt(2)}$ =1745 Hz, $P^{1/2}$) ppm. $^{195}Pt\{^1H\}$ NMR (thf-d_8, 295 K, 86 MHz): δ –3761 (m, Pt^1), –4235 (m, Pt^2), ppm.

Synthesis of $[(C_6F_5)_2Pt(\mu\text{-}PPh_2)_2Pd(dppf)]$ (2).

Method a. To an Et_2O solution (2 mL) of *cis*-$[(C_6F_5)_2Pt(PPh_2H)_2]$ (0.150 g, 0.166 mmol) was added at 195 K of *n*-LiBu (0.21 mL, 0.332 mmol). The yellow solution was stirred for 20 min and then $[Pd(dppf)Cl_2]$ (0.122 g, 0.166 mmol) was added and allowed to react at the same temperature for 2 h. After that the solution was filtered through celite at low temperature and then was evaporated to dryness. The residue was dissolved in CH_2Cl_2 (2 mL), at 273 K. The addition of cold ^{i}PrOH (3 mL) caused the crystallization of **2** as an orange solid, which was filtered off, washed with cold *i*-PrOH (2 × 2 mL) and vacuum-dried. Yield: 0.104 g, 40%.

Method b. To a yellow solution of $[NBu_4]_2[(C_6F_5)_2Pt(\mu\text{-}PPh_2)_2Pd(\mu\text{-}Cl)_2Pd(\mu\text{-}PPh_2)_2Pt(C_6F_5)_2]$ (0.250 g, 0.097 mmol) in acetone (10 mL) was added dppf (0.108 g, 0.195 mmol). The resulting orange solution was stirred at room temperature for 1 h and the complex **2** crystallized as an orange solid, which was filtered, washed with acetone (2 × 2 mL) and vacuum-dried. Yield: 0.203 g, 67%.

IR (Nujol, cm^{-1}): 1160 (ws), 864 (s), 820 (s) dppf; 953 (vs) (Fermi res.), 784 (vs), 773 (vs) (X-sensitive C_6F_5 group). Anal. Found (Calcd for $C_{70}H_{48}F_{10}FeP_4PdPt$): C, 53.82 (53.88); H, 3.08 (3.10). ^1H NMR (thf-d_8, 295 K, 400 MHz): δ 3.90 (s, $C_\beta H$, 4 H), 4.27 (s, $C_\gamma H$, 4 H), from 6.5 to 7.8 (m, Ph, 40 H) ppm. ^{19}F NMR (CD_2Cl_2, 295 K, 376.5 MHz): δ –115.1 (broad, 4 *o*-F, $^3J_{F,Pt(1)}$ = 325 Hz), –166.2 (m, 4 *m*-F), –166.4 (broad t, $^3J_{F,F}$ = 19 Hz, 2 *p*-F) ppm. $^{31}P\{^1H\}$ NMR (CD_2Cl_2, 295 K, 162 MHz): δ 13.6 (m,

$^2J_{P(3),P(1)} = {}^2J_{P(4),P(2)}$ = 262 Hz, $^2J_{P(3),P(4)}$ = 58 Hz, $^2J_{P(3),P(2)} = {}^2J_{P(4),P(1)}$ = 1 Hz), –98.2 (m, $^2J_{P(1),P(3)} = {}^2J_{P(2),P(4)}$ = 262 Hz, $^2J_{P(1),P(2)}$ = 162 Hz, $^2J_{P(1),P(4)} = {}^2J_{P(2),P(3)}$ = 1 Hz, $^1J_{P,Pt(1)}$ = 1722 Hz, $P^{1/2}$) ppm. $^{195}Pt\{^1H\}$ NMR (CD_2Cl_2, 295 K, 86 MHz): δ –3610 (m), ppm.

Synthesis of $[(PPh_3)(C_6F_5)Pt(\mu\text{-}PPh_2)_2Pt(dppf)][ClO_4]$ (3)

$[Ag(OClO_3)(PPh_3)]$ (0.049 g, 0.10 mmol) was added to a yellow solution of **1** (0.082 g, 0.05 mmol) in CH_2Cl_2 (5 mL). The mixture was stirred in the dark at room temperature for 24 h and filtered through celite. The yellow solution was evaporated to *ca*. 1 mL, ^{i}PrOH (5 mL) was added. **3** crystallized as a yellow solid, which was filtered off, washed with ^{i}PrOH (2 × 2 mL) and vacuum-dried. Yield: 0.074 g, 80.3%. IR (Nujol, cm^{-1}): 842 (s), 820 (s) (dppf); 954 (vs) (Fermi res. C_6F_5), 782 (vs) (X-sensitive C_6F_5 group), 1091 (vs), 623 (vs) (ClO_4^-). Anal. Found (Calcd for $C_{82}H_{63}ClF_5FeO_4P_5Pt_2$): C, 53.18 (53.42); H, 3.49 (3.44). Λ_M = 132 $ohm^{-1}cm^2mol^{-1}$ (acetone), ^{1}H NMR (acetone-d_6, 295 K, 400 MHz): δ 4.42 (s, $C_\beta H$, 2 H), 4.34 (s, $C_{\beta'}H$, 2 H), 4.20 (s, $C_\gamma H$, 2 H), 3.80 (s, $C_\gamma H$, 2 H), from 6.6 to 7.8 (m, *Ph*, 55 H). ^{19}F NMR (acetone-d_6, 295 K, 376.5 MHz) δ –116.2 (2 *o*-F, $^3J_{F,Pt(1)}$ = 237 Hz), –164.9 (m, 2 *m*-F), –165.0 (m, *p*-F). $^{31}P\{^1H\}$ NMR (acetone-d_6, 295 K, 162 MHz): δ 19.9 (d, PPh_3, $^2J_{P(5),P(1)}$ = 335 Hz, $^1J_{P(1),Pt(1)}$ = 2271 Hz, P^5), 16.5 (d, $^2J_{P(3),P(1)}$ = 283 Hz, $^2J_{P(3),P(4)}$ = 12 Hz, $^1J_{P(3),Pt(2)}$ = 2162 Hz, P^3), 12.5 (d, $^2J_{P(4),P(2)}$ = 289 Hz, $^2J_{P(4),P(3)}$ = 12 Hz, $^1J_{P\text{-}Pt(2)}$ = 2270 Hz, P^4), –128.7 (m, $^2J_{P(1),P(5)}$ = 335 Hz, $^2J_{P(1),P(3)}$ = 283 Hz, $^2J_{P(1),P(2)}$ = 182 Hz, $^1J_{P(1),Pt(2)}$ = 2182 Hz, $^1J_{P(1),Pt(1)}$ = 1874 Hz, P^1), –138.5 (d, $^2J_{P(2),P(4)}$ = 289 Hz, $^2J_{P(2),P(1)}$ = 182 Hz, $^1J_{P(2),Pt(2)}$ = 1954 Hz, $^1J_{P(2),Pt(1)}$ = 1660 Hz, P^2). $^{195}Pt\{^1H\}$ NMR (acetone-d_6, 295 K, 86 MHz): δ –4069 (m, Pt^1), –4238 (m, Pt^2) ppm. **Synthesis of $[(I)(C_6F_5)Pt(\mu\text{-}PPh_2)_2Pt(dppf)]$ (4).**

To a yellow solution of **1** (0.100 g, 0.06 mmol) in CH_2Cl_2 (5 mL) at 273 K was dropped I_2 (0.020 g, 0.078 mmol) in CH_2Cl_2 (2 mL). The mixture was stirred at 273 K for 24 h.

The yellow suspension was reduced a *ca*. 1 mL, Et_2O was added. The yellow solid that crystallized (**4**) was filtered, washed with Et_2O (2 × 2 mL) and vacuum-dried. Yield: 0.070 g, 73%. IR (Nujol, cm^{-1}): 821 (s) (dppf); 949 (vs) (Fermi res.), 780 (vs) (X-sensitive mode C_6F_5). Anal. Found (Calcd for $C_{64}H_{48}F_5FeIP_4Pt_2$): C, 47.44 (47.78); H, 3.00 (3.01). ^{1}H NMR (CD_2Cl_2, 295 K, 400 MHz): δ 4.32 (s, $C_\beta H$, 2 H), 4.18 (s, $C_{\beta'}H$, 2 H), 4.14 (s, $C_\gamma H$, 2 H), 3.68 (s, $C_\gamma H$, 2 H), from 6.6 to 7.7 (m, *Ph*, 40 H). ^{19}F NMR (CD_2Cl_2, 295 K, 376.5 MHz) δ –116.0 (2 *o*-F, $^3J_{F,Pt(1)}$ = 296 Hz), –166.3 (m, 2 *m*-F), –166.6 (t, $^3J_{F,F}$ = 19 Hz, *p*-F). ^{31}P{^{1}H} NMR (CD_2Cl_2, 295 K, 162 MHz): δ 15.1 (d, $^2J_{P(3),P(1)}$ = 290 Hz, $^2J_{P(3),P(4)}$ = 12 Hz, $^1J_{P(3),Pt(2)}$ = 2240 Hz, P^3), 12.3 (d, $^2J_{P(4),P(2)}$ = 246 Hz, $^1J_{P(4),Pt(2)}$ = 2116 Hz, P^4), –116.8 (m, $^2J_{P(1),P(3)}$ = 290 Hz, $^2J_{P(2),P(4)}$ = 246 Hz, $^1J_{P(1),Pt(2)}$ = 1812 Hz, $^1J_{P(1),Pt(1)}$ = 2713 Hz, $^1J_{P(2),Pt(2)}$ = 1786 Hz, $^1J_{P(2),Pt(1)}$ = 1639 Hz, overlapped P^1 and P^2). ^{195}Pt{^{1}H} NMR (CD_2Cl_2, 295 K, 86 MHz): δ –4298 (m, Pt^1), –3930 (m, Pt^2) ppm.

Synthesis of $[(C_6F_5)_2Pt(\mu\text{-}PPh_2)_2Pd(dppf)Ag][ClO_4]$ (5).

To a yellow solution of **2** (0.113 g, 0.072 mmol) in CH_2Cl_2 (5 mL), $[Ag(OClO_3)]$ (0.032 mg, 0.15 mmol) was added. The mixture was stirred in the dark at room temperature for 4 h and filtered through celite. The red solution was evaporated to *ca*. 1 ml and *n*-hexane (3 mL) was added. Complex **5** crystallized as a red solid, which was filtered, washed with *n*-hexane (2 × 2 mL) and vacuum-dried. Yield: 0.095 g, 75 %. IR (Nujol, cm^{-1}): 961 (s) (Fermi res. C_6F_5), 791 (s) and 780 (s) (X-sensitive mode C_6F_5), 1098 (s) and 623 (s) (ClO_4^-). Anal. Found (Calcd for $C_{70}H_{48}AgClF_{10}FeO_4P_4PdPt$): C, 47.62 (47.56); H, 2.72 (2.74). Λ_M = 121 (acetone), 4 (CH_2Cl_2) $ohm^{-1}cm^2mol^{-1}$. ^{1}H NMR ($CDCl_3$, 295 K, 400 MHz): δ 4.75 (s, $C_\beta H$, 2 H), 4.42 (s, $C_{\beta'}H$, 2 H), 4.12 (s, $C_\gamma H$, 2 H), 3.64 (s, $C_\gamma H$, 2 H), from 6.5 to 7.6 (m, *Ph*, 40 H). ^{19}F NMR (acetone-d_6, 200 K, 376.5

MHz): δ –115.8 (very broad, 1 *o*-F), δ –117.9 (very broad, 1 *o*-F),–119.6 (broad, $^{3}J_{F,Pt}$ = 304 Hz, 2 *o*-F,), –160.3 (t, $^{3}J_{F,F}$ = 20 Hz, 1 *p*-F), –161.5 (t, $^{3}J_{F,F}$ = 20 Hz, 1 *p*-F, –163.7 (m, overlapped 4 *m*-F), $^{31}P\{^{1}H\}$ NMR (acetone-d_6, 200 K, 161.97 MHz): δ 298.4 (broad, $^{1}J_{P(1),Pt}$ = 1140 Hz, P^1), 144.3 (m, $^{1}J_{P(2),Pt}$ = 1620 Hz, $^{1}J_{P(2),109Ag}$ = 250 Hz, $^{1}J_{P(2),107Ag}$ = 217 Hz, P^2), 25.9 (d, $^{2}J_{P(3),P(1)}$ = 89 Hz, $^{2}J_{P(3),Pt}$ = 130 Hz, P^3), 9.4 (m, $^{1}J_{P(4),109Ag}$ = 551 Hz, $^{1}J_{P(4),107Ag}$ = 479 Hz, P^4).

Reaction of $[(C_6F_5)_2Pt(\mu\text{-}PPh_2)_2Pd\ (dppf)]$ (2) with $[Ag(OClO_3)(PPh_3)]$

To a yellow solution of **2** (0.050 g, 0.032 mmol) in CH_2Cl_2 (10 mL), $[Ag(OClO_3)(PPh_3)]$ (0.030 g, 0.064 mmol) was added. The solution, which instantaneously turned red, was stirred at 273 K for 1 h. The red solution was evaporated to *ca*. 1 mL. The addition of *n*-hexane (3 mL) caused the precipitation of a mixture of complex $[(C_6F_5)_2Pt(\mu\text{-}PPh_2)_2Pd(dppf)Ag][ClO_4]$ (**5**) and $[Ag(PPh_3)_2][ClO_4]$ as a red solid, which was filtered, washed with *n*-hexane (2 × 2 mL) and vacuum-dried. Complex **5** was identified in this mixture by multinuclear NMR.

X-ray Structure Determinations

Crystal data and other details of structure analyses are collected in Table 4. Suitable crystals of **3**·CH_2Cl_2, **4**·2CH_2Cl_2, **5**·CH_2Cl_2·*n*-hexane were obtained by slow diffusion of *n*-hexane into CH_2Cl_2 (**3**, **4** and **5**) solutions of the complex. The crystals were mounted at the end of quartz fibres in a random orientation and held in place with a fluorinated oil. In all cases the diffraction data were collected with a Bruker Smart Apex diffractometer. The diffraction frames were integrated using the SAINT package [49] and corrected for absorption with SADABS [50]. The radiation used in all cases was graphite-monochromated Mo Kα (λ = 0.71073 Å).

The structures were solved by direct methods. All non-hydrogen atoms of the complexes were assigned anisotropic displacement parameters and refined without positional constraints. H atoms were added at calculated positions with equivalent isotropic displacement parameters set equal to 1.2 times those of the corresponding parent atoms. Areas of residual electron density were modelled as lattice solvent (**3:** half a molecule of CH_2Cl_2, **4:** two molecules of CH_2Cl_2, **5:** a molecule of CH_2Cl_2. In addition, an analysis of the solvent region in **5** has been performed using the SQUEEZE program [51] and, as a result, a molecule of *n*-hexane was added to the calculations). Final difference electron density maps showed some peaks above 1 e $Å^{-3}$, all of them are close to the heavy metal atoms with no chemical meaning or in the solvent areas. The structures were refined using the SHELXL-97 program [52]. Full-matrix least-squares refinement of these models against F^2 converged to the final residual indices reported in Table 4.

Appendix A. Supplementary data

CCDC 1462886, 1462887 and 1462888 contain further details of the structure determinations of **3**·0.5CH_2Cl_2, **4**·2CH_2Cl_2 and **5**·CH_2Cl_2·*n*-hexane, respectively, in CIFformat. These data can be obtained free of charge via http://www.ccdc.cam.ac.uk/conts/retrieving.html, or from the Cambridge Crystallographic Data Centre, 12 Union Road, Cambridge CB2 1EZ, UK; fax: (+44) 1223-336-033; or e-mail: deposit@ccdc.cam.ac.uk. Other supplementary data ($^{31}P\{^1H\}$ NMR spectra of **1**, **3** and **4**) can be found, in the online version.

ACKNOWLEDGMENTS. This work was supported by Ministerio de Economia y Competitividad (MINECO)/FEDER (project number CTQ2015-67461-P) and the Gobierno de Aragón (Grupo Consolidado E21: Química Inorgánica y de los

Compuestos Organometálicos). The Politecnico di Bari is gratefully acknowledged for financial support. S. I. gratefully acknowledges the grant provided by the Programma Europa CAI (CB 28/07).

Table 4. Crystal data and structure refinement for $[(C_6F_5)(PPh_3)Pt(\mu\text{-}PPh_2)_2Pt(dppf)](ClO_4)\cdot 0.5CH_2Cl_2$ (**3**$\cdot 0.5CH_2Cl_2$), $[(C_6F_5)(I)Pt(\mu\text{-}PPh_2)_2Pt(dppf)]\cdot 2CH_2Cl_2$ (**4**$\cdot 2CH_2Cl_2$) and $[(C_6F_5)_2Pt(\mu\text{-}PPh_2)_2Pd(dppf)Ag](ClO_4)\cdot CH_2Cl_2\cdot$ *n*-hexane (**5**$\cdot CH_2Cl_2\cdot$*n*-hexane).

	3·0.5CH_2Cl_2	**4·2CH_2Cl_2**	**5·CH_2Cl_2·*n*-hexane**
formula	$C_{82.5}H_{64}Cl_2F_5FeO_4P_5Pt_2$	$C_{66}H_{52}Cl_4F_5FeIP_4Pt_2$	$C_{77}H_{64}AgCl_3F_{10}FeO_4P_4Pd\ Pt$
M_t [g mol^{-1}]	1886.12	1778.69	1938.72
T [K]	100(2)	100(2)	100(2)
λ [Å]	0.71073	0.71073	0.71073
cryst syst	triclinic	monoclinic	monoclinic
space group	P-1	$P2_1/n$	P2(1)/c
a [Å]	12.8154(6)	12.8234(7)	19.4137(10)
b [Å]	13.1017(6)	19.9297(11)	14.2827(8)
c [Å]	22.3411(11)	24.2562(13)	27.3530(15)
α [deg]	90.258(1)	90	90
β [deg]	95.393(1)	101.608(1)	90.857(1)
γ [deg]	105.900(1)	90	90
V [Å^3]	3589.9(3)	6072.3(6)	7583.6(7)
Z	2	4	4
ρ [g cm^{-3}]	1.745	1.946	1.698
μ [mm^{-1}]	4.338	5.680	2.777
F(000)	1854	3424	3824

2θ range [deg]	1.66 -26.27	1.33-25.00	1.61-25.00
no. of reflns collected	30787	46486	39741
no. of unique reflns	14361	10700	13309
R(int)	0.0498	0.1365	0.0524
Final R indices [I>2σ(I)]	R1 = 0.0451, wR2 = 0.0836	R1 = 0.0665, wR2 = 0.1434	R1 = 0.0596, wR2 = 0.1590
R indices (all data)	R1 = 0.0686, wR2 = 0.0899	R1 = 0.1118, wR2 = 0.1592	R1 = 0.0764, wR2 = 0.1681
GOF on F^2	0.845	0.959	0.991

REFERENCES

[1] I. Ara, J. Forniés, S. Ibáñez, P. Mastrorilli, S. Todisco, V. Gallo, Dalton Trans., 45 (2016) 2156-2171.
[2] P. Mastrorilli, Eur. J. Inorg. Chem., (2008) 4835-4850.
[3] R. Bender, C. Okio, R. Welter, P. Braunstein, Dalton Trans., (2009) 4901-4907.
[4] C. Cavazza, F. Fabrizi de Biani, T. Funaioli, P. Leoni, F. Marchetti, L. Marchetti, P. Zanello, Inorg. Chem., (2009) 1385-1397.
[5] V. Gallo, M. Latronico, P. Mastrorilli, C.F. Nobile, G.P. Suranna, G. Ciccarella, U. Englert, Eur. J. Inorg. Chem., (2005) 4607-4616.
[6] M. Latronico, F. Polini, V. Gallo, P. Mastrorilli, B. Calmuschi-Cula, U. Englert, N. Re, T. Repo, M. Räisänen, Inorg. Chem., (2008) 9779-9796.
[7] C. Archambault, R. Bender, P. Braunstein, Y. Dusausoy, J. Chem. Soc., Dalton Trans., (2002) 4084-4090.
[8] J. Forniés, C. Fortuño, S. Ibáñez, A. Martín, Inorg. Chem. , 45 (2006) 4850-4858.
[9] I. Ara, J. Forniés, C. Fortuño, S. Ibáñez, A. Martín, P. Mastrorilli, V. Gallo, Inorg. Chem. , 47 (2008) 9069-9080.
[10] J. Forniés, C. Fortuño, S. Ibáñez, A. Martín, Inorg. Chem., 47 (2008) 5978-5987.
[11] A. Albinati, F. Balzanot, F. Fabrizi de Biani, P. Leoni, G. Manca, L. Marchetti, S. Rizzato, U.G. Barretta, Inorg. Chem., 49 (2010) 3714-3720.
[12] J. Forniés, C. Fortuño, S. Ibáñez, A. Martín, P. Mastrorilli, V. Gallo, Inorg. Chem., 50 (2011) 10798-10809.
[13] J. Forniés, C. Fortuño, S. Ibáñez, A. Martín, P. Romero, P. Mastrorilli, V. Gallo, Inorg. Chem., 50 (2011) 285-298.
[14] A. Arias, J. Forniés, C. Fortuño, S. Ibáñez, A. Martín, P. Mastrorilli, V. Gallo, S. Todisco, Inorg. Chem., 52 (2013) 11398-11408.
[15] J. Forniés, C. Fortuño, S. Ibáñez, A. Martín, P. Mastrorilli, V. Gallo, A. Tsipis, Inorg. Chem., 52 (2013) 1942-1953
[16] E. Alonso, J.M. Casas, F.A. Cotton, X. Feng, J. Forniés, C. Fortuño, M. Tomás, Inorg. Chem., 38 (1999) 5034-5040.
[17] E. Alonso, J. Forniés, C. Fortuño, A. Martín, A.G. Orpen, Organometallics., 22 (2003) 5011-5019.
[18] E. Alonso, J. Forniés, C. Fortuño, A. LLedós, A. Martín, A. Nova, Inorg. Chem., 48 (2009) 7679-7690.
[19] M. Latronico, S. Sánchez, A. Rizzuti, V. Gallo, F. Polini, E. Lalinde, P. Mastrorilli, Dalton Trans., 42 (2013) 2502–2511.
[20] T.J. Colacot, Platinum Metals Rev., 45 (2001) 22-30.
[21] Y.C. Neo, J.J. Vittal, T.S.A. Hor, J. Chem. Soc., Dalton Trans., (2002) 337-342.
[22] P. Teo, L.L. Koh, T.S.A. Hor, Inorg. Chem., 42 (2003) 7290-7296.
[23] C. Herrera-Álvarez, V. Gómez-Benítez, R. Redón, J.J. García, S. Hernández-Ortega, R.A. Toscano, D. Morales-Morales, J. Organomet. Chem., 689 (2004) 2464-2472.
[24] J. Ruiz, V. Rodríguez, A. Pérez, G. López, D. Bautista, J. Organomet. Chem., 689 (2004) 2080-2086.
[25] V. Vajpayee, H. Kim, P.S. Mukherjee, P.J. Stang, M.H. Lee, H.K. Kim, K.-W. Chi, Dalton Trans., 40 (2011) 3112-3115.
[26] S. Bivaud, S. Goeb, V. Croué, P.I. Dron, M. Allain, M. Sallé, J. Am. Chem. Soc., 135 (2013) 10018-10021.

[27] N. Chaouche, J. Forniés, C. Fortuño, A. Kribii, A. Martín, P. Karipidis, A.C. Tsipis, C.A. Tsipis, Organometallics., 23 (2004) 1797-1810.
[28] J. Forniés, C. Fortuño, R. Navarro, F. Martínez, A.J. Welch, J. Organomet. Chem., 394 (1990) 643-658.
[29] R. Usón, J. Forniés, Adv. Organomet. Chem., 28 (1988) 219-297.
[30] E.J. Maslowsky, Vibrational Spectra of Organometallics Compounds, Wiley, New York, 1997.
[31] L.R. Falvello, J. Forniés, C. Fortuño, F. Martínez, Inorg. Chem., 33 (1994) 6242-6246.
[32] E. Alonso, J. Forniés, C. Fortuño, M. Tomás, J. Chem. Soc., Dalton Trans., (1995) 3777-3784.
[33] E. Alonso, J. Forniés, C. Fortuño, A. Martín, A.G. Orpen, Organometallics., 20 (2001) 850-859.
[34] L.R. Falvello, J. Forniés, C. Fortuño, F. Durán, A. Martín, Organometallics., 21 (2002) 2226-2234.
[35] A. Arias, J. Forniés, C. Fortuño, A. Martín, M. Latronico, P. Mastrorilli, S. Todisco, V. Gallo, Inorg. Chem., 51 (2012) 12682-12696.
[36] P. Mastrorilli, S. Todisco, A. Bagno, V. Gallo, M. Latronico, C. Fortuño, D. Gudat, Inorg. Chem., 54 (2015) 5855–5863.
[37] G. Bandoli, A. Dolmella, Coord. Chem. Rev., 209 (2000) 161-196.
[38] J. Forniés, F. Martínez, R. Navarro, E.P. Urriolabeitia, Organometallics., 15 (1996) 1813-1819.
[39] A. Arias, J. Forniés, C. Fortuño, A. Martin, P. Mastrorilli, V. Gallo, M. Latronico, S. Todisco, Eur. J. Inorg. Chem., (2014) 1679-1639.
[40] G. Aullón, P. Alemany, S. Álvarez, J. Organomet. Chem., 478 (1994) 75-82.
[41] E. Alonso, J. Forniés, C. Fortuño, A. Martín, A.G. Orpen, Organometallics 19 (2000) 2690-2697.
[42] J. Forniés, C. Fortuño, S. Ibáñez, A. Martín, A.C. Tsipis, C.A. Tsipis, Angew. Chem., Int. Ed., 44 (2005) 2407-2410.
[43] I. Ara, N. Chaouche, J. Forniés, C. Fortuño, A. Kribii, A.C. Tsipis, Organometallics., 25 (2006) 1084-1091.
[44] N. Chaouche, J. Forniés, C. Fortuño, A. Kribii, A. Martín, P. Karipidis, A.C. Tsipis, C.A. Tsipis, J. Organomet. Chem., 692 (2007) 1168-1172.
[45] R. Bender, P. Braunstein, A. Dedieu, Y. Dusausoy, Angew. Chem., Int. Ed., 28 (1989) 923-925.
[46] T.J. Colacot, R.A. Teichman, R. Cea-Olivares, J.G. Alvarado-Rodríguez, R.A. Toscano, W.J. Boyko, J. Organomet. Chem. , 557 (1998) 169-179.
[47] G.P.C. Dekker, A. Buijs, C.J. Elsevier, K. Vrieze, Organometallics., 11 (1992) 1937-1948.
[48] F.T. Lapido, G.K. Anderson, Organometallics., 13 (1994) 303-306.
[49] Brucker Analytical X- Ray Systems., Madison, WI, 1998.
[50] G.M. Sheldrick, SADABS empirical absorption program, University of Göttingen, Germany, 1996.
[51] A.L. Spek, Acta Crystallogr., C71 (2015) 9-18.
[52] G.M. Sheldrick, Acta Crytallogr, Sect A., 64 (2008) 112-122.

Scheme for Table of contents

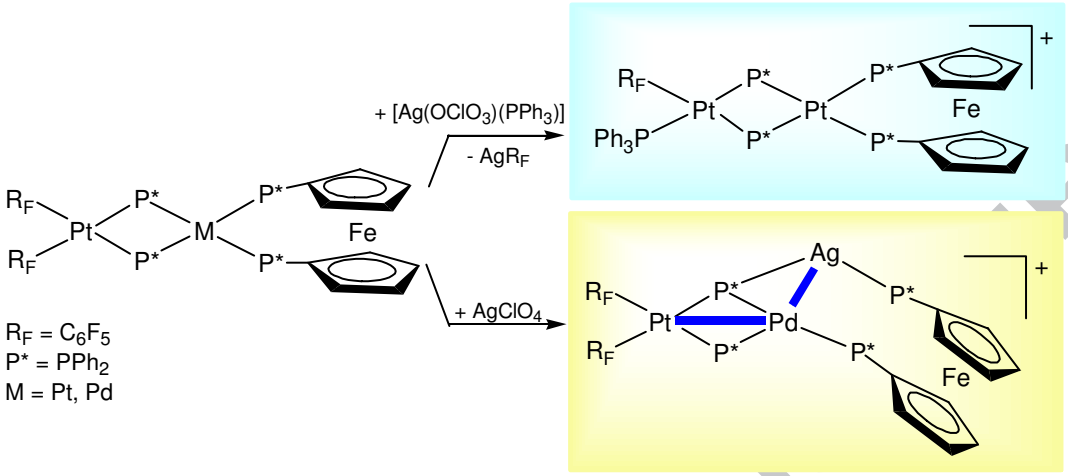

Graphical Abstracts:
Synopsis:
The behaviour of $[Ag(OClO_3)(PPh_3)]$ or $Ag(ClO_4)$ towards $[(C_6F_5)_2Pt(\mu\text{-}Ph_2)_2M(1,1'\text{-bis(diphenylphosphino)ferrocene})]$ is strongly dependent on M. Ag^+ can act as : a) C_6F_5 scavenger (M=Pt) or : b) an electrophile which produces insertion of Ag^+ into the Pd-P bond and forms a tetranuclear derivative with Pd- Ag and Pd-Pt bonds (M= Pd).